Journal of Nuclear Materials 386–388 (2009) 958–962

Contents lists available at ScienceDirect

Journal of Nuclear Materials

journal homepage: www.elsevier.com/locate/jnucmat

Experimental investigation of the IFMIF target mock-up

N. Loginov [a,*], A. Mikheyev [a], V. Morozov [a], Yu. Aksenov [a], M. Arnol'dov [a], L. Berensky [a], V. Fedotovsky [a], V. Chernov [b], H. Nakamura [c]

[a] SSC RF IPPE, Obninsk, 249033, Kaluga Region, Russia
[b] VNIINM, Moscow 123098, Russia
[c] JAEA, Tokai-mura, Ibaraki 319-1195, Japan

A B S T R A C T

The international fusion materials irradiation facility (IFMIF) lithium neutron target mock-ups have been constructed and tested at water and lithium test facilities in the IPPE of Russia. Jet velocity in both mock-ups was up to 20 m/s. Calculations and experiments showed lithium flow instability at conjunction point of straight and concave sections of the mock-up back wall. Water velocity profile across the mock-up width, jet thickness, and wave height were measured. The significant increase of thickness of both water and lithium jets near the mock-up sidewalls was observed. The influence of shape of the nozzle outlet part on jet stability was investigated. Lithium evaporation from the jet free surface was investigated as well as lithium deposition on vacuum pipe walls of the target mock-up. It was shown that these phenomena are not very critical for the target efficiency. The possibility of lithium denitration down to 2 ppm (at 10 ppm requested) by means of aluminium getter was shown. Two types of cold traps and plug indicators of impurities were tested. The results are presented in the paper.

1. Introduction

The international fusion materials irradiation facility (IFMIF) neutron target is a flat lithium jet 260 mm wide and 25 mm thick. The jet thickness should be constant in the range of ±1 mm, i.e. allowable full wave height on the surface should not exceed 2 mm. The target back wall has curvilinear shape along lithium flow and flat one in width. The back wall upper part at length of 90 mm is flat not only in width, but also along flow. Then it is mated smoothly with cylindrical part, whose curvature radius is 250 mm.

Lithium velocity is 20 m/s. There is vacuum of 10^{-5} Pa above lithium surface in the channel. Lithium temperature at the channel input is 250 °C, at the output – 285 °C. Maximal lithium temperature inside of the jet is 400 °C. Centrifugal force at the channel curvilinear part produces pressure of about 8 kPa in lithium jet, which prevents its boiling. Deuteron beam falls on the jet central part and forms rectangular 'footprint' of 200 mm in width and 50 mm in length there.

For lithium jet stability stable operation of the lithium circulation loop on the whole is necessary. One of the main features of the loop is necessity of exhausting lithium out of the quench tank, in which pressure above lithium level is about 10^{-5} Pa, by the pump. Therefore the tank should be placed at the height ensuring hydrostatic head necessary for the pump stable operation.

Low operating temperature requires fine purification of lithium from impurities to prevent formation of solid impurities. There are else some other reasons, why these impurities are not desirable. The contents of nitrogen, oxygen, hydrogen, and carbon taken separately should not exceed 10 ppm. Especially rigid restriction (1 ppm) is imposed on tritium content. The content of structural material elements is limited too. Lithium high velocity in the target can cause erosive wear.

2. Investigating the mock-up hydrodynamics

Profiles of both velocity and pressure through jet thickness, turbulence intensity, and lithium jet thickness were calculated by means of FIDAP computer code. Computing was carried out using two-dimensional approximation (jet length and thickness). Jet width was considered infinite. This approximation is valid, certainly, only far from sidewalls. Jet thickness was defined as 'uniformity function', which is equal to unity for the computational grid cells filled with liquid and to zero for empty cells. The intermediate values correspond to cells filled partially, i.e. waves, caverns, etc.

Vector velocity field at the target rectilinear section and in zone of mating with cylindrical part is shown in Fig. 1 (left). One can see that distortion of both velocity field and jet thickness take place at the mating point. The jet disturbances at this point were afterward confirmed by testing (Fig. 1, right). Besides, Fig. 1 gives an

* Corresponding author.
E-mail address: loginov@ippe.ru (N. Loginov).

0022-3115/$ - see front matter © 2009 Elsevier B.V. All rights reserved.
doi:10.1016/j.jnucmat.2008.12.257

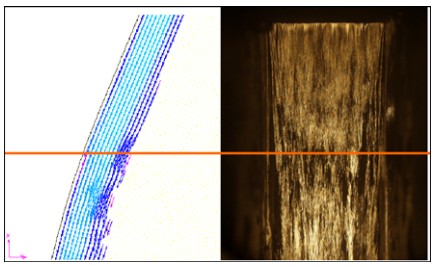

Fig. 1. Jet surface distortion (calculations and experiment).

opportunity to evaluate height of the waves arising at this place. It is equal approximately to 2mm as distance between non-disturbed streamlines is equal to 1mm. Experimental investigations were carried out at two mock-ups – 'water' mock-up and 'lithium' one.

The Shima nozzle output cross-section of the water mock-up had 76 mm width and 8 mm height. The nozzle second stage had a movable element permitting to change slightly the nozzle output shape. The test facility assured water velocity at the nozzle output up to 20 m/s. Velocity profile across the channel width at water velocity of 20 and 15 m/s was measured by the Pitot tube at different distances from the nozzle.

The velocity profile measured in three cross-sections turned out uniform except of slight velocity decrease near the channel sidewalls. The profile non-uniformity slightly increases downstream.

Electro-contact probe was used for measuring jet thickness. Its metal needle could move both across the channel width and into its depth. The needle is connected to one of power source poles; another pole is connected to the channel metal bottom. When the needle moves towards the channel bottom, electric circuit closing occurs first only at the moments of the needle contact with wave crests. Then the contacts become more long-term, their frequency increases from zero to max and again falls to zero in dipping below surface wave hollow when continuous contact is observed. The range of jet thickness variations corresponds to wave height. Jet thickness at the given point was determined by time averaging. Measurements showed that both jet thickness and wave height increased significantly near sidewalls.

To determine wave amplitude-frequency characteristics, number of contacts of liquid with the needle-electrode per time unit and relative time of the probe contact with water were measured. For example, in cross-section 1 (50 mm from the nozzle) the first contacts arise at the distance of 8.7 mm from the channel bottom, whereas circuit is continually closed at the distance of 8 mm. Thus, wave height (double amplitude) is 0.7 mm at this point of measuring, and jet local thickness is considered equal to 8.35 mm. In further increasing distance from the nozzle, jet wave height increases up to 2 mm (cross-section 3, i.e. 354 mm from the nozzle output).

Maximal frequency of contacts permits to judge about frequency of wave passage. Supposing that wave velocity is equal to flow velocity, it is possible to estimate wavelength. In the above example, wavelength is equal to 14 mm in cross-section 1, 20 mm in cross-section 2, and 28 mm in cross-section 3.

Visual examinations, photo, and video showed that ordinary surface waves had two-dimensional structure. The experiments showed that under the certain conditions other type waves arose on jet surface: periodic across the channel width structures in the form of crests and hollows oriented along the flow. In Fig. 2 left photo shows jet flowing from the nozzle at the nozzle output flat surface slope by 2 degrees towards the bottom, so as the nozzle output part along 3–5 mm length had slight divergence. Crest-shaped structures shown in this Figure have 5–6 mm height, and it essentially exceeds height of ordinary surface waves (Fig. 2, middle photo).

Fig. 2. Water jet at diverged, normal, and converged nozzle outlet.

The nozzle movable element permitted to vary smoothly angle of slope towards the channel bottom and to investigate in detail this new type of jet free surface instability. The results were reproduced repeatedly at the experimenter's request.

As the movable element sloped towards the nozzle output cross-section convergence, crest-shaped structures decreased and fully disappeared. When convergence angle became equal to 1 degree, practically smooth jet surface was observed, and even ordinary surface waves disappeared (Fig. 2, right photo).

Then the second, lithium, mock-up was installed at the water test facility (Fig. 3), in which velocity and thickness profiles and characteristics of water jet waves were measured as well. Jet thickness and range of its variations, i.e. height of waves, across the channel width are shown in Fig. 4.

At water velocity of 16 m/s wavelength is 20 mm. Wave height in these conditions is equal to 2 mm, jet average thickness is about 11 mm. Wave height and jet thickness essentially increase near sidewalls. Visual observations, photo, and video showed that water accumulated on the channel sidewalls like in Fig. 2. Jet thickness increases up to 15–20 mm there, and it is not correct to tell about wave height near the sidewalls. As a whole, hydrodynamic characteristics of the lithium mock-up are close to characteristics of the water one.

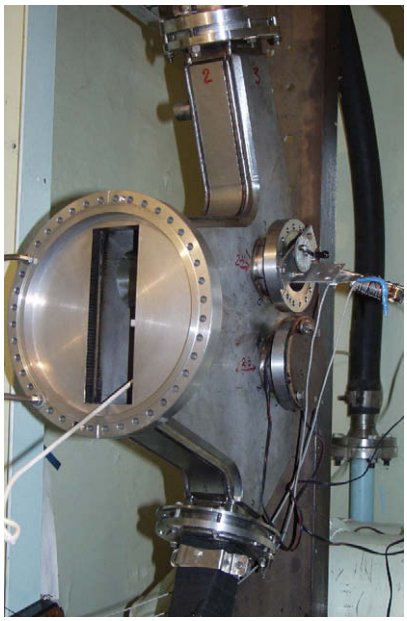

Fig. 3. Lithium mock-up at the water test facility.

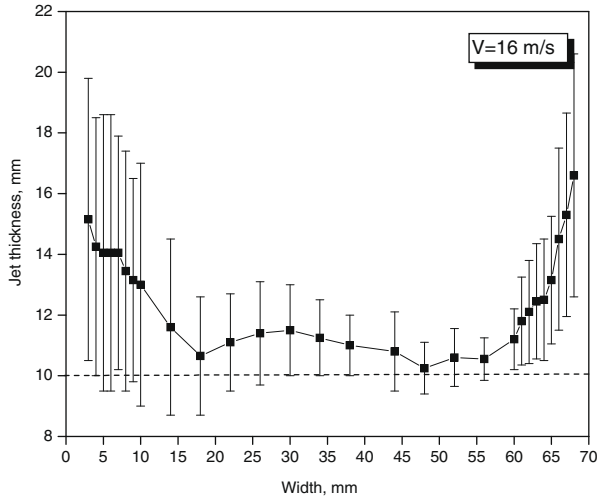

Fig. 4. The jet thickness and amplitude of surface waves across jet width at the lithium mock-up (water experiment).

Then lithium mock-up has been mounted at the LTF-M (lithium test facility modernized) designed and manufactured in the SSC RF IPPE. The LTF-M main technical specifications are as follows: lithium volume in the loop is 270 l; lithium temperature up to 400 °C; maximal lithium flow rate in the loop 50 m^3/h; pump head 0.6 MPa; maximal lithium velocity in the target mock-up 20 m/s; pressure in the mock-up vacuum cavity and quench tank 10^{-3} Pa; electric power 200 kW; the test facility height 15.6 m. Lithium level in the quench tank is about 12 m above electromagnetic pump input.

The available test facility LTF was attached to the LTF-M in order to investigate both lithium purification and methods of monitoring impurities. Lithium volume in the LTF is about 100 l, operating temperature up to 600 °C, lithium flow rate 10 m^3/h. Cold trap, sampler-distiller, plug indicator, and pipe sampler are installed at the test facility. The united flow diagram of the LTF-M and LTF lithium loops corresponds nearly completely to flow diagram of the IFMIF lithium loop.

Besides, the rotating disk facility (RD) was prepared to carry out corrosion and erosion testing structure materials in lithium. The RD facility has its own very small circulation loop for lithium purification and monitoring impurities.

The lithium mock-up is shown in Fig. 3, its main details are shown in Fig. 5. The Shima nozzle input cross-section is 70×100 mm^2, output one 70×10 mm^2, and the nozzle wall roughness about 3.2 μm. The channel back wall has concave section with radius of 250 mm and two straight sections: input section of 90 mm in length and output one of 200 mm. Leaving the channel, lithium enters the quench tank, in which lithium jet kinetic energy is being quenched.

Fig. 5. Main elements of lithium mock-up.

Before startup of lithium circulation, preparatory technological operations were carried out at the test facility: vacuum baking and then 'wet' pumping-out with lithium circulation through bypass line omitting the mock-up.

The first filling the mock-up with lithium was performed under vacuum of about 3 Pa. Video shooting lithium jet was performed during start-up of circulation through the mock-up till reaching steady-state flow condition. Transient process lasted ~0.8 s. Lithium flow was accompanied with cavitation phenomena because of gas release from steel into lithium jet, with forming bubbles and their bursting in the mock-up accompanied with sharp sound effects. This process was recorded by video. Injection of argon into the mock-up and gradual increase of its pressure up to ~7 kPa caused disappearing cavitation. Like in water tests, flowing lithium film over the mock-up sidewalls was observed. This lithium film began from the nozzle edge and under the gravitation influence flowed vertically down till its junction with jet. The tests in vacuum were performed at lithium velocity up to ~10 m/s. Higher velocity caused cavitation. Most of the investigations were carried out in argon atmosphere in the velocity range of 7–20 m/s, under absolute argon pressure of 93–94 kPa, and at lithium temperature of 300–325 °C.

When operating with maximal flow rate (50.8 m^3/h), appearance of lithium foam from the quench tank was observed in the target mock-up. When flow rate decreased to 19 m^3/h, the foam disappeared. The foam appearance conditions were reproduced repeatedly.

To validate the target serviceability, it is important to know both rate of lithium evaporation from jet surface and deposition in vacuum path. Experiments and corresponding calculations were carried out for this purpose.

Lithium supplied by manufacturers contains up to 0.1% (mass) of impurities. Sodium and potassium impurities are the most volatile at the temperature of 250–300 °C. Partial pressure of components of highly diluted solutions of sodium and potassium in lithium is described by the Raoul's law. Calculations show that pressure of sodium and lithium vapors are of the same order when sodium concentration is 0.01% (mass).

Free-moleculte regime of vapor flow takes place in both the IFMIF target and lithium mock-up work conditions. Modified Hertz–Knudsen's formula [1] was used to estimate mass transfer. Table 1 presents comparison of lithium, sodium, and potassium evaporation rates from jet surface according to calculation and experimental results [2]. The calculated values (column 2) in the Table show mass transfer rate at the beginning and end of the time interval investigated. A good match between the results of computing and experiment for sodium and potassium was obtained. As for lithium, the reason of tenfold discrepancy of the results demands clarification.

Distribution of deposition growth rate along the vacuum path obtained experimentally by the authors is shown in Fig. 6. For this purpose special experimental section was attached to the target mock-up opposite to jet free surface. Both calculations and experiments showed that lithium evaporation and deposition in the vacuum path are not very critical for the target operation.

Table 1
Comparison of calculated and experimental [3] mass transfer rates, g/day.

Component	Calculation	Experiment
Sodium	0.91…0.82	0.895
Potassium	1.4×10^{-3}…8.3×10^{-4}	7.3×10^{-4}
Lithium	2.6×10^{-2}	0.241

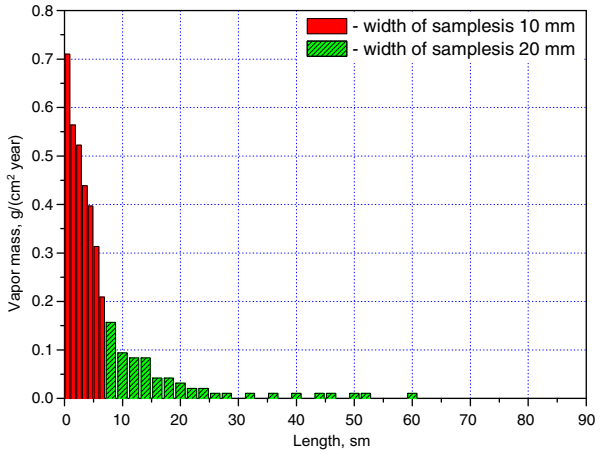

Fig. 6. Lithium deposition rate along vacuum path.

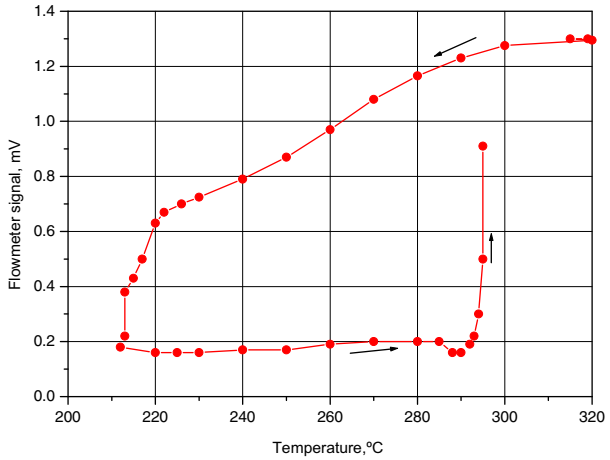

Fig. 7. Plugging diagram before purification.

3. Lithium purification and monitoring impurities

The known three-zone trap cooled by water [3] was used at the LTF. Lithium flow rate through the trap was about 0.5 m^3/h. The trap total volume was about 10 l. Lithium temperature at the trap input was 230–250 °C, and 190–200 °C at its output. Diffusive disk trap was installed at the RD. The RD cold trap volume was about 1.5 l. These traps were cooled either by air or by water. Lithium temperature at their input was 230–250 °C, and 190–210 °C at the output.

The traps showed effective enough purification from oxygen and hydrogen. For instance, the RD disc trap purified the loop of 4 l in volume for 4 h. The temperature at the trap output was 205–210 °C. Oxygen concentration before purification was 14 ppm, hydrogen one was 83 ppm. After purification they were 5.5 and 50, correspondingly. It is known that lithium purification from nitrogen by cold traps is not effective. Therefore getter methods of purification are of interest.

The authors researched lithium purification from nitrogen by aluminium dissolved. Purification was performed in a tank with lithium, in which about 0.3% (mass) of aluminium was added. Lithium in the tank was mixed during about an hour at 300 °C. Then lithium was filtered, and sample was taken for analyzing. Initial nitrogen content in lithium was 50–100 ppm (in different tests). After purification, concentration diminished down to 2–5 ppm. Lithium purification by aluminium was also performed in the RD facility circulation loop. Plug indicator temperature of plugging was 300 °C before purification (concentration of saturation with nitrogen was 8700 ppm). After adding 0.9% (mass) of aluminium, plugging temperature diminished down to ~190 °C, and chemical analysis of the samples showed nitrogen concentration of 1.6–6.0 ppm. Aluminium nitride was eliminated from the loop by filtration or settling in the tank.

The authors used sampler-distiller, plug indicator, electrochemical cell and pipe sampler for monitoring impurities in lithium.

The sampler-distiller design for oxygen control is well known. Distillation of twenty-gram probe was carried out during five hours at 750 °C.

Zirconium dioxide electrochemical cell with indium reference electrode was used at the RD facility. It is known that zirconium dioxide dissociates in lithium at 300 °C and above. Since the IFMIF temperature is 250–285 °C, it was decided to test the cell. By means of this cell, wetting stainless steel with lithium at 240 °C was observed. Besides, thermodynamic potential of oxygen in lithium was first measured within the temperature range from melting point to 320 °C, and oxygen concentration in lithium was estimated before and after cold trapping.

Two plug indicators were tested successfully. They showed not only one, but also two or even three plugging temperatures. The most interesting information was obtained while testing new indicator design at the RD facility. The feature of the indicator is uniting in one design of both plugged orifices with magnetic flowmeter channel and the flowmeter electrodes with thermocouples. The flowmeter signal was measured between identical thermocouple electrodes. The orifice plugged, or the flowmeter channel, is a narrow annular gap of 6 mm in diameter and 0.5 mm in width.

Fig. 7 shows plugging diagram of the indicator. Flow rate decrease was observed at the temperatures of 300, 220, and 212 °C. It is supposed that these temperatures are saturation ones for nitrogen, oxygen and hydrogen, correspondingly. They correspond to 8700, 14 and 83 ppm. Washing out the indicator occurred at 295 °C. After 4 hours of cold trapping, the first plugging was observed at 295 °C, the second one at 190 °C (line 1, Fig. 8), and washing out at 210 °C. Steadiness of the first plugging temperature (295 °C) is an evidence of the nitrogen plugging, because it is known that cold trap catches nitrogen poorly. Decrease of the second plugging temperature from 220 down to 190 °C is an evidence of oxygen and hydrogen concentration decrease.

After aluminium getter purification, indicator shows only one plugging temperature, namely 190 °C (line 2). It is plugging with oxygen and/or hydrogen. Their concentrations are $\leqslant$5.5 ppm and $\leqslant$50 ppm, correspondingly. Disappearance of the first plugging temperature is an evidence of purification of lithium from nitro-

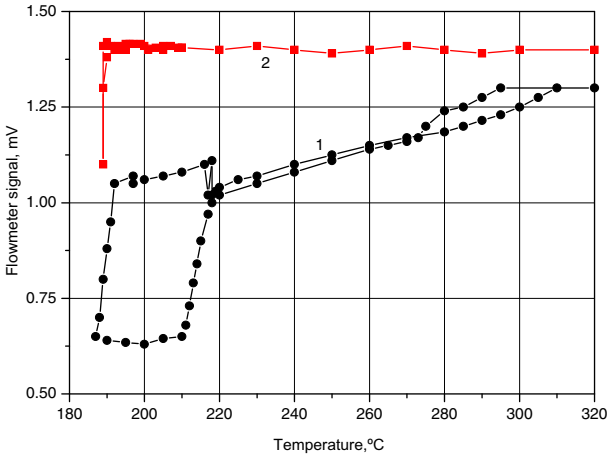

Fig. 8. Plugging diagram after 4-h purification (1) and aluminium gettering (2).

gen. Analysis of lithium from the pipe sampler showed 1.6–6.0 ppm of nitrogen. Thus, it is shown that plug indicators can be used successfully at test lithium facilities and can be adapted for the IFMIF.

4. Discussion

The calculated and experimental investigations of hydrodynamics of the IFMIF lithium target mock-up showed that at the point of conjunction of back wall rectilinear part with its cylindrical part jet instability arose due to sudden change of centrifugal force acting on lithium. To avoid this phenomenon, it is necessary to exclude the back wall rectilinear part and use either parabolic or cylindrical profile. In the first case centrifugal force will continuously increase and then decrease along the mock-up length. In the second case centrifugal force will be constant along all length of the back wall.

The experiments at the water mock-up showed that shape of the Shima nozzle output part influenced essentially jet stability. Slight divergence of this part (angle of 1–2 degrees) together with the dulled nozzle edge causes generation of waves in the form of crests and hollows of very large amplitude (5–6 mm) located along the jet. On the contrary, slightly converged outlet part (angle of 0.5–1 degree) essentially increases jet stability and decreases surface waves down to their full disappearance. Both in water and in lithium tests, trickling liquid thin film vertically down along sidewalls is observed beginning from the nozzle output. It is caused by the fact that jet velocity on the wall is equal to zero, inertia force is absent, and liquid film moves under influence of gravity. Good wettability of the wall by lithium increases this effect.

At the part of the target with cylindrical back wall, liquid accumulates on its sidewalls, and jet thickness near them increases doubly in comparison with the central part. The reason is decreasing centrifugal force near sidewalls to zero and displacing liquid from the channel central part to the walls. The width of these wall layers increases downstream and generates large amplitude waves on jet surface.

At initial stage of operation of the lithium circulation loop under vacuum conditions, significant gas release from steel was observed. It caused generation of bubbles in lithium, their bursting in the mock-up, and cavitation in the pump. Despite the loop previous degassing, it continued for two weeks. Similar phenomena were observed at the ELS [4] test facility for about two months because the test facility was not, probably, previously degassed.

The investigations of intensity of lithium evaporation from jet surface showed that this process would not be critical for the IFMIF operation. But content of such impurities as sodium and especially potassium should be rigidly limited.

The possibility of lithium purification from oxygen to the required concentration of less than 10 ppm by cold trap was confirmed by experiments. The possibility of purification from nitrogen by aluminium to the same concentration was also shown. Development of methods of purification from hydrogen to required concentration remains urgent.

It seems expedient to have first of all plug indicator among facilities of monitoring impurities in the IFMIF lithium loop as the most simple and reliable device showing temperature of lithium saturation with impurities. It will permit to decide if purification of lithium is necessary (plugging temperature $\geqslant 250\ ^\circ C$) or not (plugging temperature is less, for instance, 230 °C). The indicator construction can be improved to get automatically operated device.

Other devices for monitoring separately oxygen, hydrogen, and nitrogen need further development.

5. Conclusions

The hydrodynamic and technological researches carried out showed that the IFMIF lithium target and circulation loop could be serviceable. Some improvements are proposed and some questions are pointed out.

The created complex test facility LTF−M + LTF practically completely reproduces (in reduced scale) the IFMIF lithium circulation loop and can be used to go on investigating lithium hydrodynamics and technology for validation of both the IFMIF project and prototype test facility at the experimental validation and engineering design activity (EVEDA) stage. The RD facility can be used for corrosion/erosion tests of materials.

Acknowledgements

The authors express their sincere gratitude to the ISTC for financing and organizational support of the work performed on Project No. 2036.

References

[1] M.N. Ivanovsky, V.P. Sorokin, V.I. Subbotin, Evaporation and condensation of metals – M.: Atomizdat, 1976 (in Russian).
[2] N.I. Loginov, M.N. Arnol'dov, V.S. Fedotovsky et al. The thermal-hydraulic and technological investigations for validation of the project of lithium circulation loop and neutron lithium target for IFMIF: Final Report. No. 47-11/341, 2006.
[3] V.I. Subbotin, M.N. Arnol'dov, M.N. Ivanovsky, A.A. Mosin, A.A. Tarbov. Lithium. – M.: IzdAt, 1999 (in Russian).
[4] R. Kolowith, J.D. Berg, W.C. Miller, Experimental lithium system: final report, HEDL-TME-84-29, 1985.